Electronic Supplementary Material (ESI) for Physical Chemistry Chemical Physics.

Electronic Supplementary Information

Experimental and computational methods

Preparation of bulk g-C_3N_4

Typically, bulk g-C_3N_4 was synthesized by directly heating 10.0 g dicyandiamide in muffle furnace from room temperature to 550°C for 4 h with the ramp rate of 15°C/min.

Preparation of bulk g-C_3N_4 with different heating time

5.0 g dicyandiamide was firstly heated from room temperature to 400°C for 30 min with the ramp rate of 15°C/min. The sample kept for 0 min and 30 min was marked as 400-0 min and 400-30 min, respectively. Then the temperature was raised to 550°C with the ramp rate of 15°C/min. The samples kept for 15 min, 30 min, 45 min, 60 min and 120 min were denoted as 550-15 min, 550-30 min, 550-45 min, 550-60 min, and 550-120 min, respectively.

Preparation of g-C_3N_4 nanorods

In a typical synthesis, 5.0 g of dicyandiamide were spread on the bottom of porcelain boat.[1] The precursors were heated independently using an infrared hot plate (IR 4000, Fisher Scientific). The power was determined as 50% and the heating time was 2 h. The measurement results show that the final temperatures for 50% was 560 °C. The resulting solid on the bottom boat was thoroughly ground with an agate mortar and then collected.

Preparation of MOF doped g-C_3N_4 nanorods

The preparation procedure of MOF coordinated g-C_3N_4 was conducted as follow: 10.0 g of dicyandiamide and different mass of [1, 1'-Bis (diphenylphosphino) ferrocene] dichloropalladium (II) was added into mortar.[2] The samples adding 10 mg, 25 mg, and 50 mg MOF were denoted as 10 mg, 25 mg, and 50 mg, respectively. After being milled for 5 min, the precursors were transferred to porcelain boat covered with aluminum foil. If 15 mL water was added into the porcelain boat, the product is denoted as W and the addition of ethanol is denoted as E. If the step is omitted, the product is denoted as N.

The infrared hot plate was operated as previously reported. The precursors were heated for 2 h at different power levels and the obtained g-C_3N_4 were transferred to 80 °C oven immediately. Samples treated at 50% and 80% power are denoted as 50%P and 80%P, respectively. Take N-50 mg-80%P for example, no solvent and 50 mg MOF was added into the dicyandiamide, and the precursor was heated at 80% power for 2 h. Notably, the measurement results show that the final temperature for 50% and 80% was respectively 520 °C and 600 °C, and they are also the most commonly used temperature in other experiments. The heating rate was more than 50 °C/min. The product was then collected and thoroughly ground with an agate mortar prior to characterization. All chemicals are of analytical grade and were used without further purification.

Preparations of oxidized g-C_3N_4

Porous g-C_3N_4 were synthesized via the chemical oxidation of bulk g-C_3N_4 with $K_2Cr_2O_7$-H_2SO_4 as previously reported.[3]10.0 g of $K_2Cr_2O_7$ was mixed with 50 mL H_2SO_4 (98 wt%) in a 100 mL flask and stirred until the solution became brown. Different mass of bulk g-C_3N_4 was added to the solution and stirred for 2 h at room temperature. The samples adding 0.25 g, 0.50 g, 1.0 g, 5.0 g, and 15 g were denoted as 0.25-Oxi-C_3N_4, 0.50-Oxi-C_3N_4, 1.0-Oxi-C_3N_4, 5.0-Oxi-C_3N_4, and 15-Oxi-C_3N_4 respectively. The mixture was slowly poured into 500 mL of deionized water and cooled to room temperature. After centrifugation at 5000 rpm, the obtained solid was dialyzed in a dialysis bag to remove all residual acids. Finally, the obtained suspension was vacuum dried and the milk-white solid were collected.

Photocatalytic activity

The photocatalytic activity was evaluated by degrading 10 mg/L Rhodamine B (RhB) aqueous solution under ultraviolet light (300 W Xe lamp). Typically, 50 mg product was dispersed into 50 mL dye solution in a 100 mL quartz reactor with a circulating water system keeping 20.0 °C. A 304 W (19 V × 16 A) Xe lamp with 420 nm cutoff filter was used when irradiating the turbid liquid. Prior to the photodegradation, the suspension was stirred at 1000 rpm in the dark for 1 h to reach the adsorption equilibrium. The suspension was collected at given time intervals (10 min) and the concentration was determined by the UV-vis spectrophotometer at 553 nm.

Computational Methods

D-spacing Calculation for Hexagonal. The d-spacing corresponding to specific hkl in hexagonal unit cell is calculated as:

$$\frac{1}{d^2} = \frac{4}{3}\left(\frac{H^2 + HK + K^2}{a^2}\right) + \frac{L^2}{c^2} \qquad (1)$$

where d is the crystal plane spacing, hkl the crystal face index, abc the cell parameters.

Reflection Intensity. The intensity of (hkl) reflection in XRD is determined as:

$$I_{hkl} = KL_p\left|F_{hkl}\right|^2 = \frac{1 + \cos^2 2\theta}{\sin^2 \theta\cos\theta}KF\cdot F^* = \frac{1 + \cos^2 2\theta}{\sin^2 \theta\cos\theta}K\left\{\left[\sum_j f_j\cos 2\pi\left(hx_j + jy_j + lz_j\right)\right]^2 + \left[\sum_j f_j\sin 2\pi\left(hx_j + jy_j + lz_j\right)\right]^2\right\} \qquad (2)$$

where K is the planar multiplicity factor and mainly related to the scanning mode (absorption factor) and temperature

(Debye-Waller factor), L_p the Lorentz polarization factor with θ being the Bragg angle of (hkl) reflection, F_{hkl} the structure factor and a complex function. Besides, the stress distribution in powder was omitted, which may cause changes in peak profiles. The relative intensity was calculated dividing by the intensity of (002) peak. In all the calculations, the dependence of the atomic-scattering factor on the value of sin θ/λ =1/2d is considered.

Data Smoothing for XRD patterns. The least-squares smoothing and differentiation by Savitzky-Golay (SG) method is carried out when smoothing the patterns.[4]

$$\bar{I}_i = \sum_{j=1}^{m} C_j I_{[i+j-(m+1)/2]} \Big/ \sum_{j=1}^{m} C_j \qquad (3)$$

where I_i is the initial intensity, $_i$ the smoothed intensity, m the number of data points participated in data smoothing and set at 11 in the calculation (11 pts), C_j the weight factor for each data point. The convolution weights for quadratic initial points are set at -36/429, 6/429, 44/429, 69/429, 84/429, 89/429, 84/429, 69/429, 44/429, 9/429, -36/429 from I_{i-5} to I_{i+5}, respectively.

The least-squares smoothing and differentiation by SG method is also used in the smoothed second derivative, as shown in Equation 4. [4]

$$\bar{I}_i = \sum_{n=-(m-1)/2}^{n=(m-1)/2} C_n I_{[i+n]} \qquad (4)$$

m is also set at 11 (11 pts) and the convolution weights are set at 15/429, 6/429, -1/429, -6/429, -9/429, -10/429, -9/429, -6/429, -1/429, 6/429, 15/429, respectively.

By the way, the baseline corrections are carried out by Shirley method.

Discrete Fourier expansion. To avoid physical meaningless fitting functions (such as Cauchy Function, Gauss Function, Voigt Function, pseudo-Voigt Function, Pearson VII Function etc.), discrete Fourier transform (also referred to as fast Fourier transform, or FFT) is used to give a method with straightforward theoretical significance. Any functions meeting the Dirichlet condition can be expressed by Fourier series, thus the broad diffraction peaks can be transformed into Fourier series expansion:

$$I(2\theta) = \frac{A_0}{2} + \sum_{n=1}^{2N+1}\left[A_n\cos\left(\frac{2\pi n}{2N}2\theta\right) - B_n\sin\left(\frac{2\pi n}{2N}2\theta\right)\right] \qquad (5)$$

where 2N is the hits and equal to 100 in following calculations, A_0, A_n, B_n the Fourier coefficients and can be calculated as:

$$A_0 = \frac{1}{N}\sum_{1}^{101} I(2\theta)\Delta(2\theta) \tag{6}$$

$$A_n = \frac{1}{N}\sum_{1}^{101} I(2\theta)\cos\left(\frac{2\pi n}{2N}2\theta\right)\Delta(2\theta) \tag{7}$$

$$B_n = \frac{1}{N}\sum_{1}^{101} I(2\theta)\sin\left(\frac{2\pi n}{2N}2\theta\right)\Delta(2\theta) \tag{8}$$

where n =1, 2, 3 …

Extraction of the peak profile. The obtained separated diffraction peak can be further corrected as shown:[5]

$$H(t) = \sum_{2\theta} h(2\theta)e^{-4\pi i\theta t/a} \tag{9}$$

$$G(t) = \sum_{2\theta} g(2\theta)e^{-4\pi i\theta t/a} \tag{10}$$

$$F(t) = \sum_{2\theta} f(2\theta)e^{-4\pi i\theta t/a} \tag{11}$$

where h (2θ) is the measured shape patterns of the peak, g (2θ) the shape patterns of the instrument, f (2θ) the theoretical shape patterns of the peak. H (t), G (t), and F (t) are the corresponding Fourier transform functions.

According to Fourier transform theory, there is:

$$H(t) = F(t)G(t) \tag{12}$$

And the Fourier transform function is the combination of real part and imaginary part. For example:

$$G(t) = \sum_{2\theta} g(2\theta)\cos(4\pi\theta t/a) + i\sum_{2\theta} g(2\theta)\sin(4\pi\theta t/a) = G_r(t) + iG_i(t) \tag{13}$$

where the G_r (t) represents for the real part while G_i (t) the imaginary part.

Thus, the F (t) can be calculated as:

$$F(t) = \frac{H(t)}{G(t)} = \frac{H_r(t) + iH_i(t)}{G_r(t) + iG_i(t)} = \frac{(H_r + iH_i)(G_r - iG_i)}{G_r^2 + G_i^2} \tag{14}$$

And the theoretical patterns f (2θ) can be recalculated as:

$$f(2\theta) = \sum_t \frac{H(t)}{G(t)}e^{-4\pi i\theta t/a} = \sum_t [F_r(t) + F_i(t)][\cos(4\pi\theta t/a) - i\sin(4\pi\theta t/a)] \tag{15}$$

The real part of the Fourier transform function can represent for f (2θ).

$$f(2\theta) = \sum_t [F_r(t)\cos(4\pi\theta t/a) + F_i(t)\sin(4\pi\theta t/a)] \tag{16}$$

Resolving overlapping peaks. Assuming that the broad peak around 12°-14° consists of two peaks, and one can be described as:[6]

$$I_1(2\theta) = \frac{a_0}{2} + \sum_{n=1}^{101}\left[a_n\cos\left(\frac{2\pi n}{2N}2\theta\right) - b_n\sin\left(\frac{2\pi n}{2N}2\theta\right)\right] \tag{17}$$

Thus the total diffraction patterns can be described as:

$$I(2\theta) = I_1(2\theta) + RI_1(2\theta - \Delta 2\theta) = I_1(2\theta) + I_1(2\theta - \Delta 2\theta) \tag{18}$$

where R is the intensity ratio of the two peaks and is assumed to be 1 for simplicity. Δ2θ is the resolution of two peaks. Herein, we hypothesize that the two diffraction peaks share the same peak profile, width and intensity distribution (and the assumption can be further polished up).

Hence, the Fourier coefficients for the diffraction peak can be calculated as:

$$a_0 = \frac{A_0}{1+R} = \frac{A_0}{2} \tag{19}$$

$$a_n = \frac{A_n + R\left\{A_n\cos\left[\frac{2\pi n}{2N}\Delta(2\theta)\right] + B_n\sin\left[\frac{2\pi n}{2N}\Delta(2\theta)\right]\right\}}{1 + \cos\left[\frac{2\pi n}{2N}\Delta(2\theta)\right] + R^2} = \frac{A_n + A_n\cos\left[\frac{2\pi n}{2N}\Delta(2\theta)\right] + B_n\sin\left[\frac{2\pi n}{2N}\Delta(2\theta)\right]}{2 + \cos\left[\frac{2\pi n}{2N}\Delta(2\theta)\right]} \tag{20}$$

$$b_n = \frac{B_n + R\left\{B_n\cos\left[\frac{2\pi n}{2N}\Delta(2\theta)\right] - A_n\sin\left[\frac{2\pi n}{2N}\Delta(2\theta)\right]\right\}}{1 + \cos\left[\frac{2\pi n}{2N}\Delta(2\theta)\right] + R^2} = \frac{B_n + B_n\cos\left[\frac{2\pi n}{2N}\Delta(2\theta)\right] - A_n\sin\left[\frac{2\pi n}{2N}\Delta(2\theta)\right]}{2 + \cos\left[\frac{2\pi n}{2N}\Delta(2\theta)\right]} \tag{21}$$

The fitting peak position can be obiter calculated as:

$$< 2\theta >= \sum 2\theta I(2\theta) \Big/ \sum I(2\theta) \tag{22}$$

The obtained line profile is further smoothed through SG method, thus we can get smooth curves and calculate the integral area easier.

By the way, the local maximum with threshold σ = 3.0 (confidence level at 99.85%) and width larger than 1.5 FWHM can be determined as a peak in this study.

Results and discussion

Deduction

It is widely established that the building block of g-C_3N_4 is 2,5,8-triazido-s-heptazine, and the tri-s-triazine units are in orienting ordered arrangement for ideal g-C_3N_4 crystal, as shown in Fig. S1. Although the element analysis always show that there are some hydrogen atoms (typically ca. 3%) in g-C_3N_4, the results turns out to be the defect structures such as C-NH-C bridges and C-NH_2 terminal groups in the imperfect planar structure if the polymerization degree is low. Hence, the lattice point of idea g-C_3N_4 crystal should be a heptazine together with tri-s-triazine unit, as tagged in black frame.

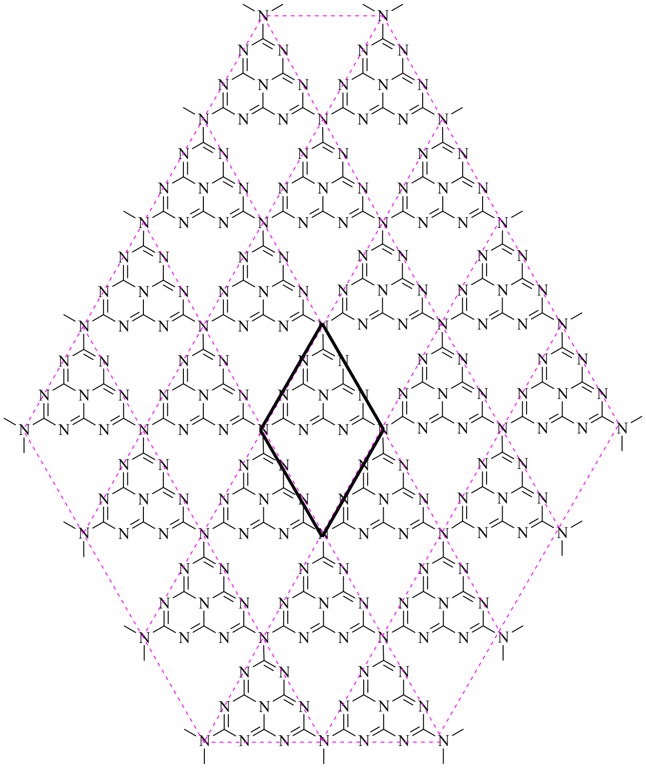

Fig. S1 The ideal 2D crystal structure of g-C_3N_4.

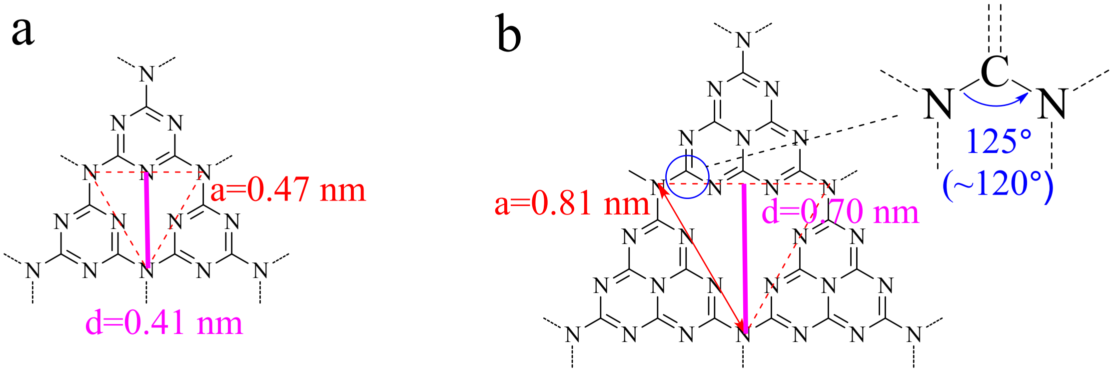

Fig. S2 Structures considered representative of g-C_3N_4: (a) triazine and (b) tri-s-triazine based.

With respect to the size of lattice point, we can calculate it by trigonometric functions. It is widely accepted that tri-s-triazine arranges in planar construction. As we can know, the covalent radius for C and N is respectively 77 pm and 75 pm, and the bond angle for C-N-C is approxiamately 120°, as shown in Fig. S2. Horvath-Bordon et al. also reported that the peripheral C–N–C angles are ca. 118° in the cyamelurate anion and 116° in tri-s-triazine, while the remaining C–N–C and N–C–N angles are 120°.[7] Hence, the theoretical distance between N-N is 1.73 times the length of C-N bond, namely 263 pm. Hence, the 3 times the length of N-N and should be 789 pm. They also reported the average N–C(O)–N angle is 125° in cyamelurate, thus the length of N-N is 270 pm and the size of tri-s-triazine is 810 pm.

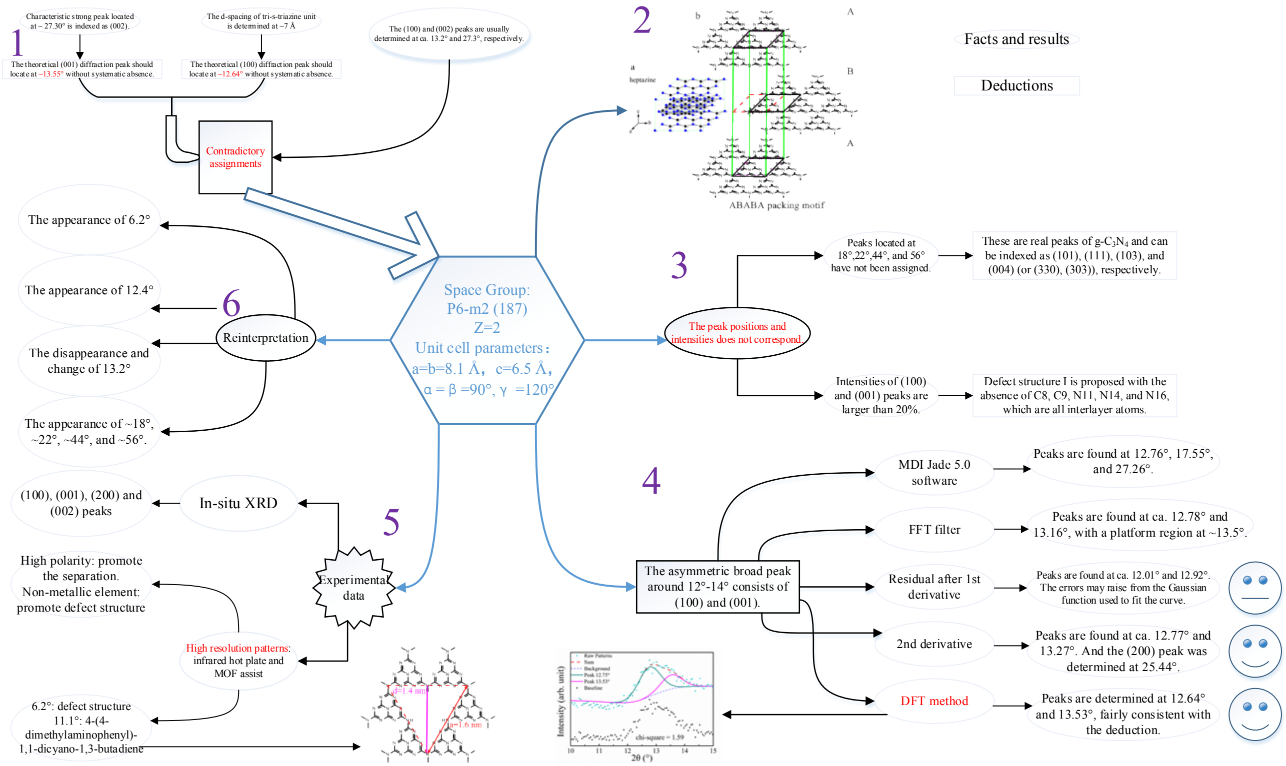

Characteristic strong peak located at ~ 27.30° is indexed as (002).

The theoretical (001) diffraction peak should locate at ~13.55° without systematic absence.

The d-spacing of tri-s-triazine unit is determined at ~7 Å

The theoretical (100) diffraction peak should locate at ~12.64° without systematic absence.

The (100) and (002) peaks are usually determined at ca. 13.2° and 27.3°, respectively.

Contradictory assignments

Facts and results

Deductions

Space Group: P6-m2 (187) Z=2 Unit cell parameters: a=b=8.1 Å, c=6.5 Å, α = β =90°, γ =120°

The peak positions and intensities does not correspond.

Peaks located at 18°,22°,44°, and 56° have not been assigned.

These are real peaks of g-C_3N_4 and can be indexed as (101), (111), (103), and (004) (or (330), (303)), respectively.

Intensities of (100) and (001) peaks are larger than 20%.

Defect structure I is proposed with the absence of C8, C9, N11, N14, and N16, which are all interlayer atoms.

The asymmetric broad peak around 12°-14° consists of (100) and (001).

MDI Jade 5.0 software

Peaks are found at 12.76°, 17.55°, and 27.26°.

FFT filter

Peaks are found at ca. 12.78° and 13.16°, with a platform region at ~13.5°.

Residual after 1st derivative

Peaks are found at ca. 12.01° and 12.92°. The errors may raise from the Gaussian function used to fit the curve.

2nd derivative

Peaks are found at ca. 12.77° and 13.27°. And the (200) peak was determined at 25.44°.

DFT method

Peaks are determined at 12.64° and 13.53°, fairly consistent with the deduction.

Experimental data

In-situ XRD

(100), (001), (200) and (002) peaks

High resolution patterns: infrared hot plate and MOF assist

High polarity: promote the separation. Non-metallic element: promote defect structure

6.2°: defect structure 11.1°: 4-(4-dimethylaminophenyl)-1,1-dicyano-1,3-butadiene

Reinterpretation

The appearance of 6.2°

The appearance of 12.4°

The disappearance and change of 13.2°

The appearance of ~18°, ~22°, ~44°, and ~56°.

Fig. S3 Illustration of the compositions and major conclusions in this article. The paper is unfolded in the order of Arabic numbers.

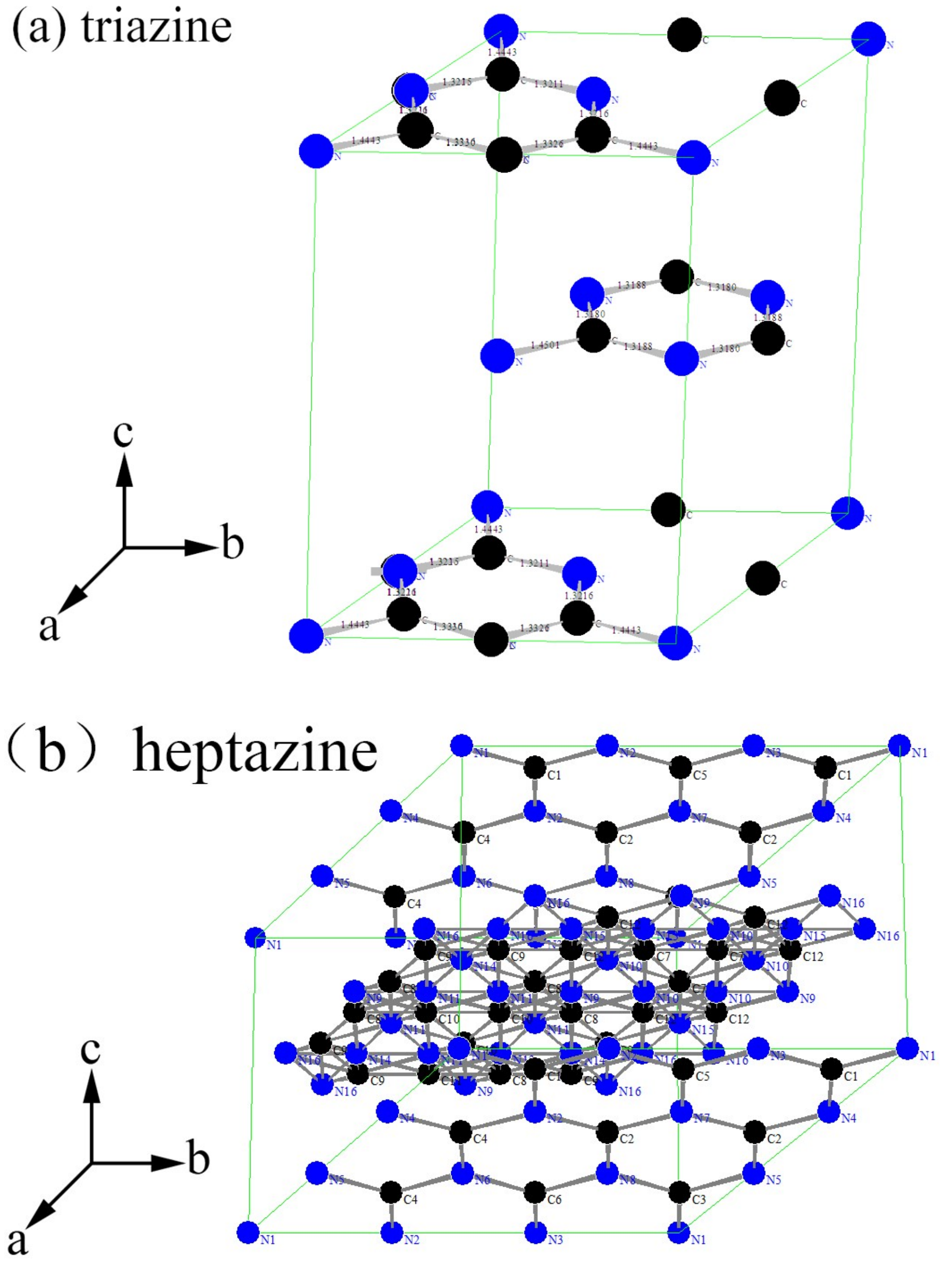

Fig. S4 The crystal structure of (a) triazine and (b) heptazine based g-C_3N_4.

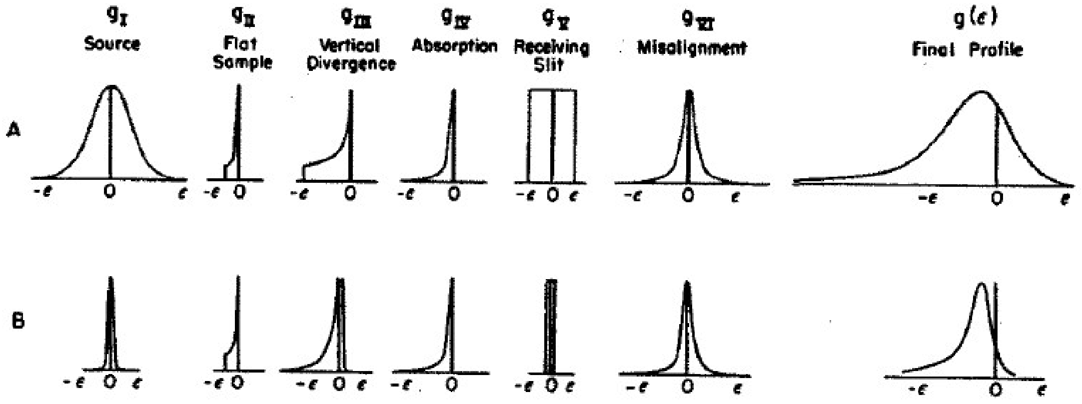

Fig. S5 The six instrumental weight functions for spectrometers of (a) old and (b) new designs computed for typical experimental conditions.[8]

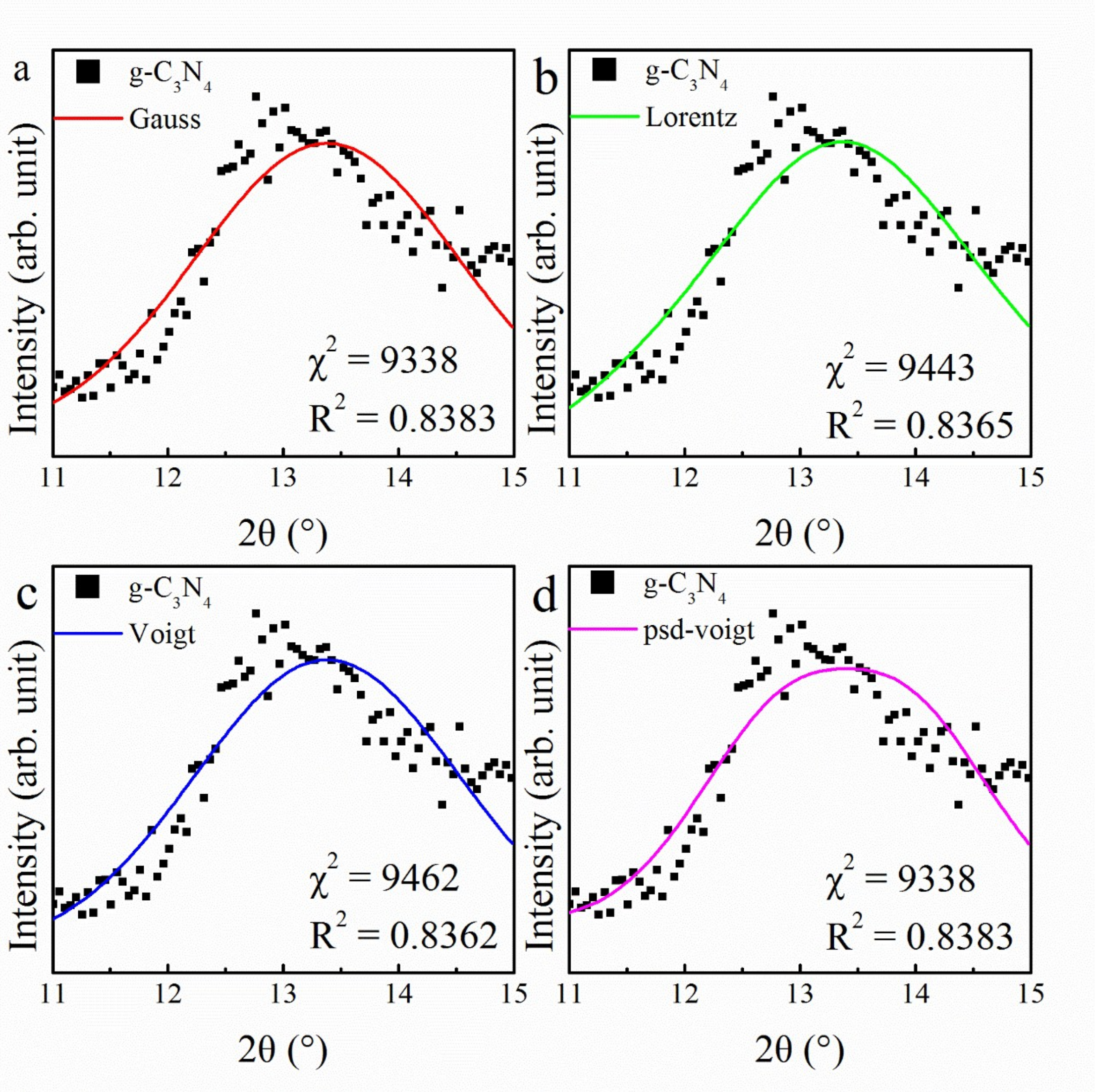

Fig. S6 The fitting results by using (a) Gauss, (b) Lorentz, (c) Voigt, and (d) PsdVoigt functions.

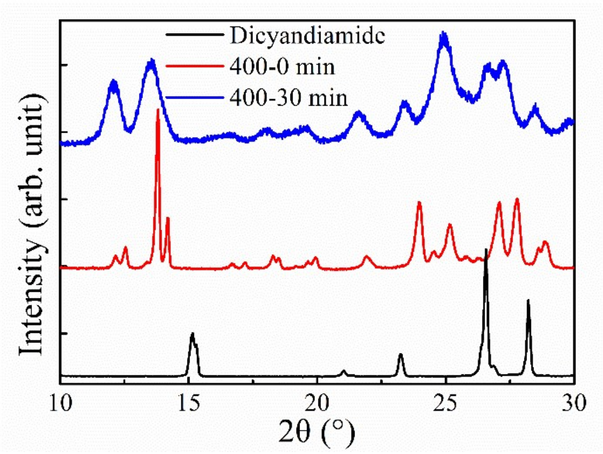

Fig. S7 XRD patterns for dicyandiamide, 400-0 min, and 400-30 min.

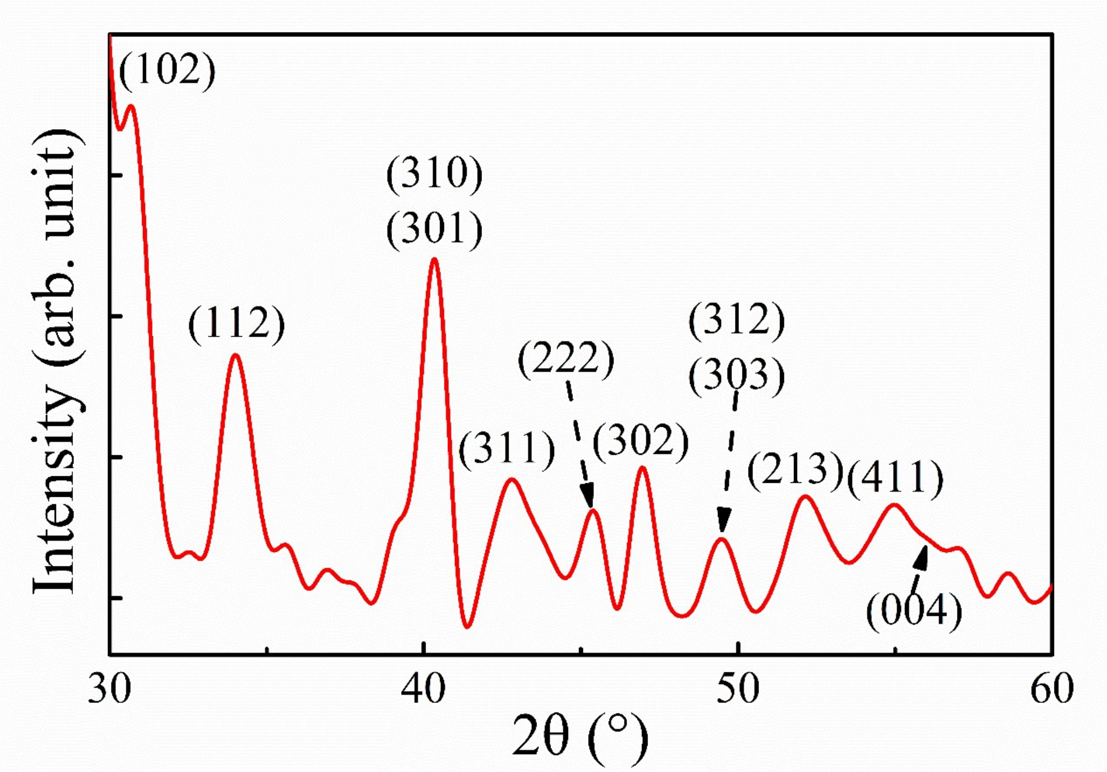

Fig. S8 Assignments to FFT Smoothed XRD patterns for N-50 mg-50%P g-C_3N_4 in large angle (30° < 2θ < 60°).

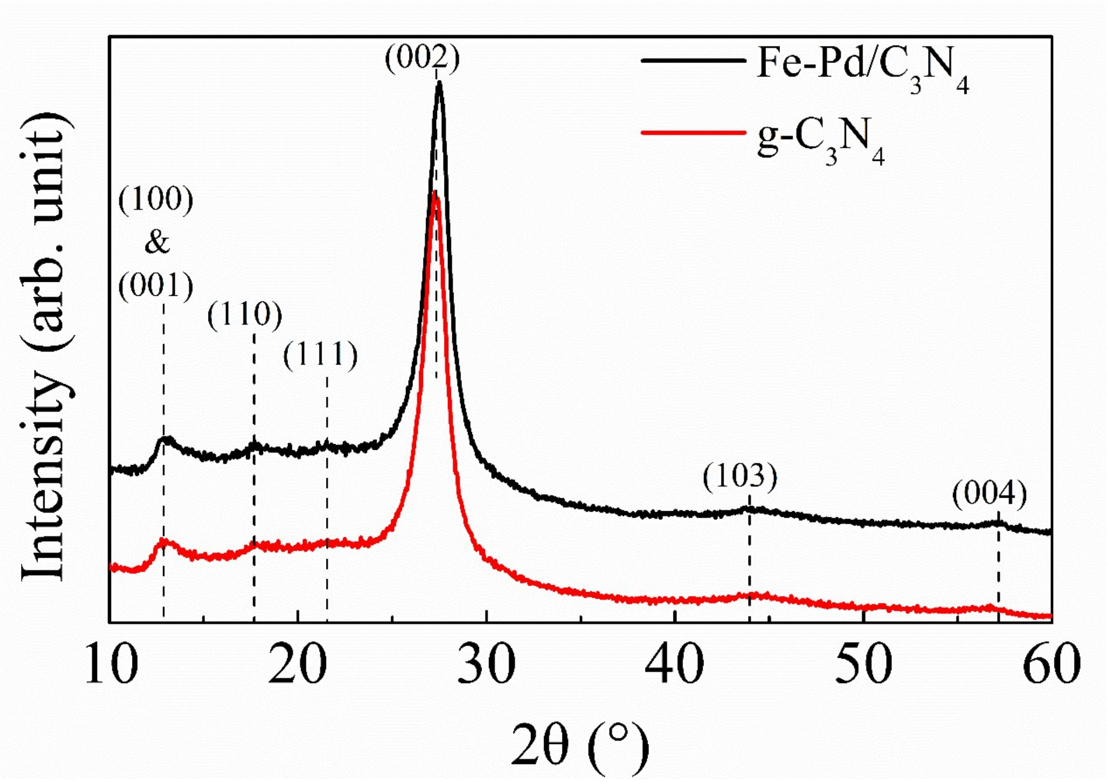

Fig. S9 XRD patterns of g-C_3N_4 and Fe-Pd/C_3N_4.

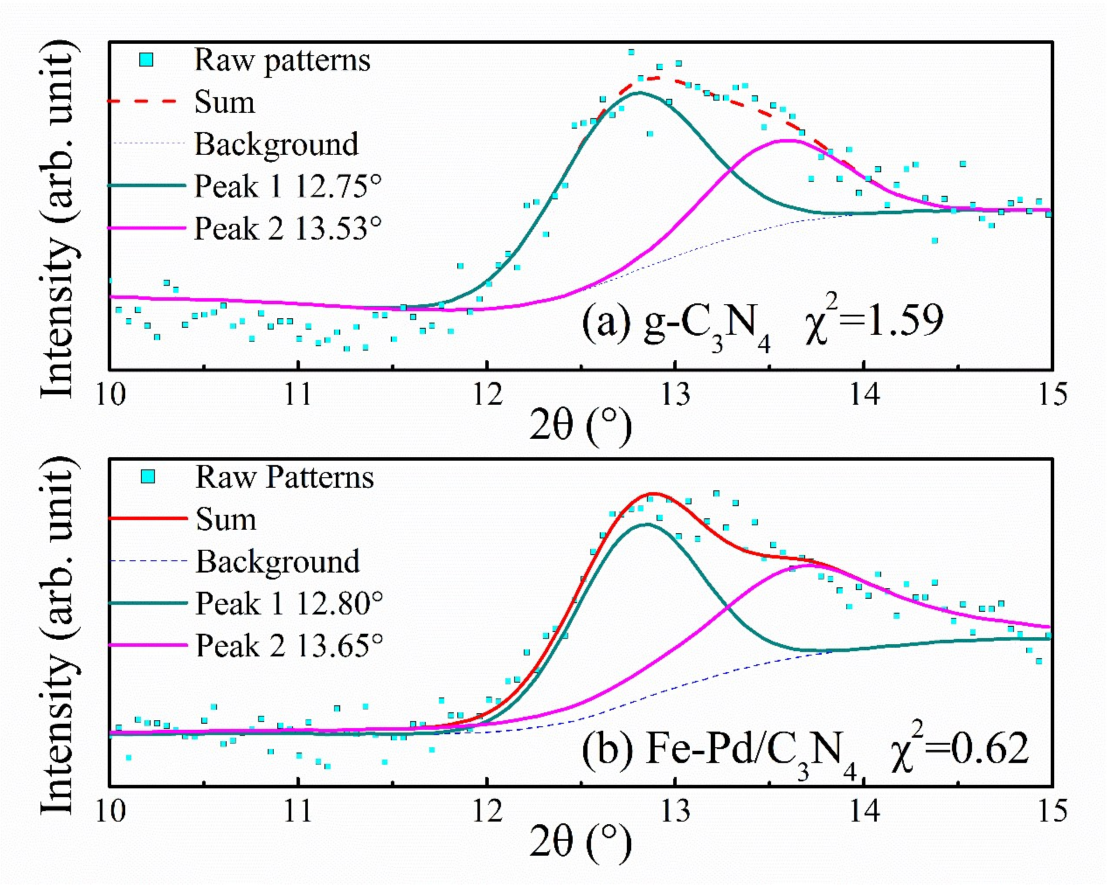

Fig. S10 DFT results of XRD patterns for (a) g-C_3N_4 and (b) Fe-Pd/C_3N_4.

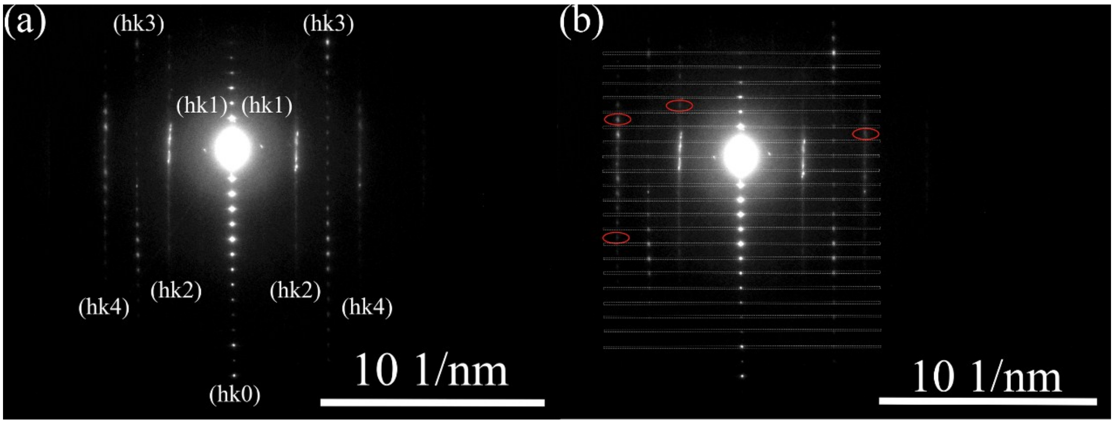

Fig. S11 (a) SAED patterns and (b) the illustration of ABA… stacking sequence for 50 mg-50%P g-C_3N_4 nanorods prepared by infrared hot plate.

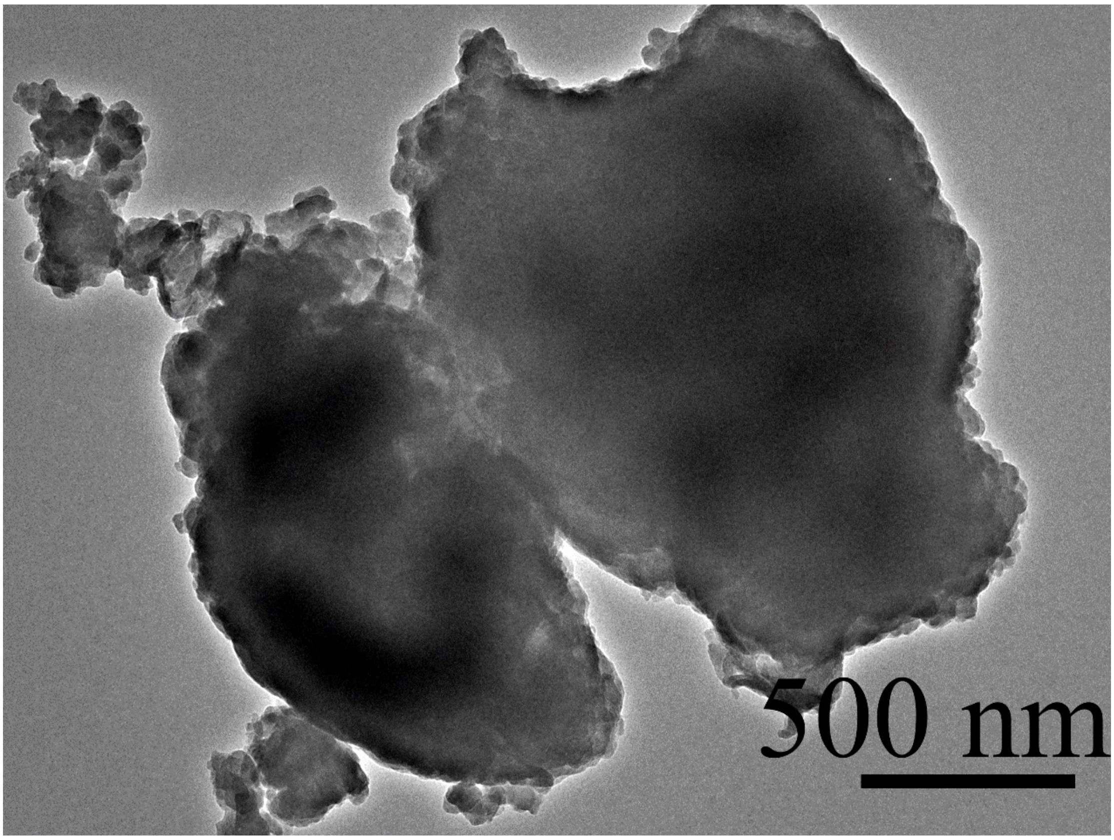

Fig. S12 TEM images of 1000-Oxi-C3N4.

Table S1 Structural parameters of triazine and heptazine based crystalline g-C_3N_4.

	triazine based g-C_3N_4	heptazine based g-C_3N_4
Space Group	Pm2 (187)	Pm2 (187)
Z	2	2
a (Å)	4.742	8.1
c (Å)	6.720	6.5
C1	3j (0.3517,0.1759.0.0000)	3j (0.8889,0.1111,0.0000)
C2	3k (0.0197,0.5099,0.5000)	3j (0.8889,0.4444,0.0000)
C3	6l (0.5000,0.0000,0.0000)	6l (0.8889,0.7778,0.0000)
C4		3j (0.2222,0.7778,0.0000)
C5		6l (0.5556,0.1111,0.0000)
C6		6l (0.5556,0.7778,0.0000)
C7		3k (0.7222,0.2778,0.0000)
C8		6m (0.0556,0.6111,0.5000)
C9		6m (0.5556,0.2778,0.5000)
C10		3k (0.3889,0.6111,0.5000)
C11		6m (0.3889,0.9444,0.5000)
C12		6m (0.3889,0.2778,0.5000)
N1	1a (0.0000,0.0000,0.0000)	1a (0.0000,0.0000,0.0000)
N2	1f (0.6667,0.3333,0.5000)	6l (0.3333,0.0000,0.0000)
N3	3k (0.1694,0.3387,0.5000)	6l (0.6667,0.0000,0.0000)
N4	3j (0.5026,0.4974,0.0000)	6l (0.0000,0.3333,0.0000)

N5	6l (0.0000,0.6667,0.0000)
N6	1c (0.3333,0.6667,0.0000)
N7	1e (0.6667,0.3333,0.0000)
N8	6l (0.6667,0.6667,0.0000)
N9	3k (0.5000,0.5000,0.5000)
N10	6m (0.8333,0.5000,0.5000)
N11	6m (0.1667,0.5000.0.5000)
N12	6m (0.5000,0.8333,0.5000)
N13	6m (0.5000,0.1667,0.5000)
N14	3k (0.1667,0.8333,0.5000)
N15	3k (0.8333,0.1667,0.5000)
N16	6m (0.1667,0.1667,0.5000)

The radius of carbon atoms is assumed to be 77 pm while 75 pm for nitrogen atoms.

Table S2 All the interplanar spacings of the g-C_3N_4 according to JCPDS and literature.

hkl	JCPDS: 87-1256			Literature: 13.2° & 27.3°		
	2θ /°	d /nm	I_f	2θ /°	d /nm	I_f
001	13.16	672.0	0.1	13.55	652.8	0
100	21.62	410.6	2.8	13.20	670.2	0
101	25.40	350.4	10.3	18.96	467.6	8.956
002	26.50	336.0	100.0	27.30	326.4	100.0
102	34.46	260.0	1.1	30.44	293.4	0
110	37.92	237.1	1.1	18.71	473.9	1.301
111	40.30	223.5	0.1	23.17	383.5	0
003	40.30	223.5	0.1	41.46	217.6	0
200	44.07	205.3	3.2	26.58	335.1	1.668
201	46.19	196.3	15.9	29.95	298.1	0
103	46.19	196.3	15.9	43.70	207.0	1.551
112	46.86	193.7	1.0	33.30	268.8	0.3368
202	52.16	175.2	3.0	38.47	233.8	0.7210
004	54.58	168.0	5.3	56.33	163.2	40.04
104	59.39	155.5	0.1	58.13	158.6	0
210	59.51	155.2	0.1	29.78	299.7	0
203	61.18	151.4	1.3	49.93	182.5	0
211	61.18	151.4	1.3	32.85	272.4	0.6422
212	66.27	140.9	0.1	40.84	220.8	0
114	68.38	137.1	0.2	59.89	154.3	0.2237

300	68.49	136.9	0.1	40.34	223.4	0
301	70.10	134.1	0.1	42.75	211.4	11.47
204	72.65	130.0	0.6	63.33	146.7	0.007607
105	74.17	127.8	0.1	73.89	128.2	0.3546
213	74.28	127.6	0.2	51.88	176.1	0.3480
302	74.83	126.8	0.1	49.39	184.4	0
220	81.05	118.6	2.6	37.94	237.0	0.2731
214	85.00	114.0	0.1	65.02	143.3	0
310	85.11	113.9	0.1	42.62	211.9	0.6255
205	86.46	112.5	0.9	78.57	121.7	0
006	86.90	112.0	0.9	90.14	108.8	
222	87.10	111.8	4.0	47.37	191.8	0.1985

Table S3 All the calculated X-ray powder-diffraction patterns (ideal and defective) of Pm2 g-C_3N_4 (a = 8.439 Å).

crystal structure				ideal		defect I		defect II	
hkl	2θ /°	d /nm	L_p	$\|F_{hkl}\|^2$	I_f	$\|F_{hkl}\|^2$	I_f	$\|F_{hkl}\|^2$	I_f
100	12.10	730.8	42.63	0	0	22.19	25.04	31.79	39.22
001	13.55	652.8	33.57	0	0	25.00	22.22	36.00	34.97
110	17.15	516.8	20.26	4.000	1.448	7.000	3.755	4.000	2.345
101	18.21	486.8	17.77	29.65	9.412	33.87	15.93	19.05	9.796
111	21.92	405.2	11.76	0	0	1.000	0.3114	0	0
200	24.34	365.4	9.28	11.26	1.867	33.30	8.182	4.219	1.133
210	27.26	326.8	7.17	0	0	1.000	0.1898	0	0
002	27.30	326.4	7.14	784.0	100.0	529.0	100.0	484.0	100.0
201	27.96	318.8	6.77	0	0	15.08	2.703	21.13	4.139
102	29.96	298.0	5.79	0	0	22.19	3.402	31.79	5.326
211	30.56	292.2	5.54	7.093	0.7020	5.852	0.8583	7.093	1.137
112	32.42	276.0	4.87	4.000	0.3480	7.000	0.9026	4.000	0.5637
220	34.69	258.4	4.22	4.000	0.3015	7.000	0.7821	4.000	0.4885
300	36.87	243.6	3.74	0	0	7.000	0.6931	9.000	0.9740
202	36.89	243.4	3.74	11.26	0.7523	33.30	3.297	4.219	0.4566
221	37.40	240.2	3.65	7.093	0.4625	1.000	0.09664	0	0
310	38.94	231.1	3.40	11.26	0.6839	5.566	0.5010	11.26	1.108
212	38.97	230.9	3.39	0	0	1.000	0.08975	0	0
301	39.45	228.2	3.33	208	12.37	139.0	12.25	133	12.82
311	41.41	217.9	3.09	0	0	1.000	0.08181	0	0

003	41.46	217.6	3.09	0	0	25.00	2.045	36.00	3.219
103	43.35	208.6	2.93	29.65	1.5520	33.87	2.627	19.05	1.615
320	44.67	202.7	2.85	11.26	0.5733	1.000	0.07546	0	0
222	44.70	202.6	2.84	4.000	0.2029	7.000	0.5263	4.000	0.3287
113	45.17	200.5	2.82	0	0.000	1.000	0.07466	0	0
302	46.48	195.2	2.77	0	0.000	7.000	0.5134	9.000	0.7214
321	46.90	193.6	2.76	29.65	1.462	21.58	1.577	29.65	2.368
312	48.21	188.6	2.73	11.26	0.5491	5.566	0.4023	11.26	0.8895
203	48.66	187.0	2.73	0	0	15.08	1.090	21.13	1.669
400	49.87	182.7	2.73	7.093	0.3459	1.837	0.1328	6.731	0.5317
213	50.34	181.1	2.73	7.093	0.3459	5.852	0.4230	7.093	0.5603
410	51.52	177.2	2.76	0	0	1.000	0.07307	0	0
401	51.93	175.9	2.77	0	0	1.723	0.1264	1.086	0.08705
330	53.13	172.3	2.81	784.0	39.36	529.0	39.36	484.0	39.39
322	53.15	172.2	2.81	0	0	1.000	0.07440	0	0
411	53.53	171.1	2.83	4	0.2022	1.000	0.07493	4.000	0.3279
331	55.10	166.6	2.91	0	0	25.00	1.9261	36.00	3.031
223	55.14	166.4	2.91	0	0	1.000	0.07704	0	0
420	56.25	163.4	2.98	29.65	1.578	21.58	1.7026	29.65	2.557
004	56.33	163.2	2.99	784.0	41.88	529.0	41.88	484.0	41.88
303	56.67	162.3	3.02	208.0	11.22	139.0	11.11	133.0	11.62
402	57.78	159.4	3.11	7.093	0.3941	1.837	0.1513	6.731	0.6058
104	57.84	159.3	3.11	0	0	22.20	1.828	31.79	2.861
421	58.15	158.5	3.14	0	0	1.000	0.08313	0	0

313	58.18	158.4	3.15	0	0	1.000	0.08340	0	0
412	59.28	155.8	3.25	0	0	1.000	0.08605	0	0
114	59.33	155.6	3.26	4.000	0.2330	7.000	0.6042	4.000	0.3773

Table S4 All the calculated X-ray powder-diffraction patterns (ideal and defective) of Pm2 g-C_3N_4 (a = 8.236 Å).

crystal structure				ideal		defect I		defect II	
hkl	2θ /°	d /nm	L_p	$\lvert F_{hkl}\rvert^2$	I_f	$\lvert F_{hkl}\rvert^2$	I_f	$\lvert F_{hkl}\rvert^2$	I_f
100	12.40	713.2	40.50	0	0	22.19	23.78	31.79	37.23
001	13.55	652.8	33.57	0	0	25.00	22.20	36.00	34.95
110	17.57	504.3	19.20	4.000	1.371	7.000	3.556	4.000	2.221
101	18.41	481.5	17.34	29.65	9.178	33.87	15.54	19.05	9.552
111	22.26	399.1	11.36	0	0	1.000	0.3006	0	0
200	24.95	356.6	8.771	11.26	1.763	33.30	7.727	4.219	1.070
002	27.30	326.4	7.145	784.0	100.0	529.0	100.0	484.0	100.0
210	27.95	319.0	6.773	0	0	1.000	0.1792	0	0
201	28.50	313.0	6.481	0	0	15.08	2.586	21.13	3.960
102	30.08	296.8	5.737	0	0	22.19	3.368	31.79	5.274
211	31.18	286.6	5.298	7.093	0.6708	5.852	0.8203	7.093	1.087
112	32.65	274.0	4.792	4.000	0.3422	7.000	0.8875	4.000	0.5543
220	35.57	252.2	4.012	4.000	0.2865	7.000	0.7430	4.000	0.4641
202	37.32	240.8	3.662	11.26	0.7361	33.30	3.226	4.219	0.4468
300	37.81	237.7	3.575	0	0	7.000	0.6621	9.000	0.9304
221	38.23	235.2	3.506	7.093	0.4439	1.000	0.09276	0	0
212	39.47	228.1	3.324	0	0	1.000	0.08794	0	0
310	39.94	225.5	3.262	11.26	0.6557	5.566	0.4804	11.26	1.062
301	40.34	223.4	3.213	208.0	11.93	139.0	11.82	133.0	12.36
003	41.46	217.6	3.090	0	0	25.00	2.044	36.00	3.217

311	42.37	213.2	3.006	0	0	1.000	0.07953	0	0
103	43.44	208.1	2.921	29.65	1.546	33.87	2.618	19.05	1.609
113	45.35	199.8	2.812	0	0	1.000	0.07440	0	0
222	45.41	199.5	2.809	4.000	0.2006	7.000	0.5202	4.000	0.3249
320	45.84	197.8	2.792	11.26	0.5612	1.000	0.07387	0	0
302	47.26	192.2	2.749	0	0	7.000	0.5091	9.000	0.7154
321	48.02	189.3	2.735	29.65	1.448	21.58	1.562	29.65	2.345
203	49.00	185.7	2.728	0	0	15.08	1.088	21.13	1.667
312	49.06	185.5	2.728	11.26	0.5484	5.566	0.4017	11.26	0.8882
213	50.75	179.8	2.740	7.093	0.3469	5.852	0.4242	7.093	0.5620
400	51.19	178.3	2.749	7.093	0.3481	1.837	0.1336	6.731	0.5351
410	52.89	173.0	2.799	0	0	1.000	0.07405	0	0
401	53.21	172.0	2.812	0	0	1.723	0.1282	1.086	0.08831
322	54.17	169.2	2.856	0	0	1.000	0.07556	0	0
330	54.54	168.1	2.876	784.0	40.25	529	40.25	484.0	40.25
411	54.86	167.2	2.894	4.000	0.2067	1.000	0.07657	4.000	0.3347
223	55.75	164.7	2.950	0	0	1.000	0.07805	0	0
004	56.33	163.2	2.990	784.0	41.85	529.0	41.85	484.0	41.85
331	56.48	162.8	3.002	0	0	25.00	1.986	36.00	3.125
303	57.36	160.5	3.072	208.0	11.41	139.0	11.30	133.0	11.81
420	57.76	159.5	3.107	29.65	1.645	21.58	1.774	29.65	2.664
104	57.92	159.1	3.121	0	0	22.20	1.833	31.79	2.869
313	58.93	156.6	3.218	0	0	1.000	0.08514	0	0
402	58.98	156.5	3.223	7.093	0.4081	1.837	0.1566	6.731	0.6273

114	59.48	155.3	3.276	4.000	0.2339	7.000	0.6067	4.000	0.3789
421	59.63	154.9	3.292	0	0	1.000	0.08710	0	0
412	60.53	152.8	3.395	0	0	1.000	0.08982	0	0

Table S5 All the calculated X-ray powder-diffraction patterns (ideal and defective) of Pm2 g-C_3N_4 (a = 7.739 Å).

crystal structure				ideal		defect I		defect II	
hkl	2θ /°	d /nm	L_p	$\|F_{hkl}\|^2$	I_f	$\|F_{hkl}\|^2$	I_f	$\|F_{hkl}\|^2$	I_f
100	13.20	670.2	38.51	0	0	22.19	22.61	31.79	35.40
001	13.55	652.8	33.57	0	0	25.00	22.20	36.00	34.95
110	18.71	473.9	18.22	4	1.301	7.000	3.374	4.000	2.107
101	18.96	467.6	16.92	29.65	8.956	33.87	15.16	19.05	9.321
111	23.17	383.5	10.98	0	0	1.000	0.2905	0	0
200	26.58	335.1	8.300	11.26	1.668	33.30	7.312	4.219	1.013
002	27.30	326.4	7.145	784	100.0	529.0	100.0	484.0	100.0
210	29.78	299.7	6.409	0	0	1.000	0.1696	0	0
201	29.95	298.1	6.211	0	0	15.08	2.478	21.13	3.795
102	30.44	293.4	5.682	0	0	22.19	3.336	31.79	5.223
211	32.85	272.4	5.072	7.093	0.6422	5.852	0.7853	7.093	1.040
112	33.30	268.8	4.717	4	0.3368	7.000	0.8736	4.000	0.5456
220	37.94	237.0	3.824	4	0.2731	7.000	0.7082	4.000	0.4423
202	38.47	233.8	3.587	11.26	0.7210	33.30	3.160	4.219	0.4376
300	40.34	223.4	3.425	0	0	7.000	0.6343	9.000	0.8914
221	40.47	222.7	3.380	7.093	0.4280	1.000	0.08942	0	0
212	40.84	220.8	3.257	0	0	1.000	0.08617	0	0
003	41.46	217.6	3.144	0	0	25.00	2.080	36.00	3.273
310	42.62	211.9	3.112	11.26	0.6255	5.566	0.4583	11.26	1.013
301	42.75	211.4	3.090	208	11.47	139.0	11.36	133.0	11.88

103	43.70	207.0	2.930	29.65	1.551	33.87	2.626	19.05	1.614
311	44.93	201.6	2.915	0	0	1.000	0.07712	0	0
113	45.85	197.8	2.804	0	0	1.000	0.07419	0	0
222	47.37	191.8	2.780	4	0.1985	7.000	0.5149	4.000	0.3216
320	48.96	185.9	2.754	11.26	0.5536	1.000	0.07286	0	0
302	49.39	184.4	2.735	0	0	7.000	0.5065	9.000	0.7118
203	49.93	182.5	2.728	0	0	15.08	1.088	21.13	1.667
321	51.05	178.8	2.728	29.65	1.444	21.58	1.558	29.65	2.339
312	51.36	177.8	2.730	11.26	0.5488	5.566	0.4020	11.26	0.8889
213	51.88	176.1	2.748	7.093	0.3480	5.852	0.4255	7.093	0.5636
400	54.74	167.6	2.785	7.093	0.3526	1.837	0.1354	6.731	0.5421
004	56.33	163.2	2.861	784	40.04	529.0	40.04	484.0	40.04
410	56.57	162.5	2.874	0	0	1.000	0.07604	0	0
401	56.67	162.3	2.915	0	0	1.723	0.1329	1.086	0.09154
322	56.96	161.5	2.965	0	0	1.000	0.07845	0	0
223	57.45	160.3	2.982	0	0	1.000	0.07890	0	0
104	58.13	158.6	2.990	0	0	22.20	1.756	31.79	2.749
330	58.37	158.0	2.995	784	41.92	529.0	41.92	484.0	41.92
411	58.46	157.7	3.117	4	0.2226	1.000	0.08247	4.000	0.3605
303	59.23	155.9	3.128	208	11.61	139.0	11.50	133.0	12.03
114	59.89	154.3	3.133	4	0.2237	7.000	0.58023	4.000	0.3624
331	60.22	153.5	3.256	0	0	25.00	2.154	36.00	3.390
313	60.97	151.8	3.292	0	0	1.000	0.08710	0	0
420	61.86	149.9	3.298	29.65	1.746	21.58	1.883	29.65	2.828

402	62.23	149.1	3.355	7.093	0.4248	1.837	0.1631	6.731	0.6530
421	63.66	146.1	3.471	0	0	1.000	0.09183	0	0
412	63.93	145.5	3.558	0	0	1.000	0.09413	0	0

Table S6 All the calculated X-ray powder-diffraction patterns (ideal and defective) of Pm2 g-C_3N_4 (a = 8.042 Å).

crystal Structure				ideal		defect I		defect II	
hkl	2θ /°	d /nm	L_p	$\lvert F_{hkl}\rvert^2$	I_f	$\lvert F_{hkl}\rvert^2$	I_f	$\lvert F_{hkl}\rvert^2$	I_f
100	12.70	696.4	38.51	0	0	22.19	22.61	31.79	35.40
001	13.55	652.8	33.57	0	0	25.00	22.20	36.00	34.95
110	18.00	492.4	18.22	4.000	1.301	7.000	3.374	4.000	2.107
101	18.61	476.3	16.92	29.65	8.956	33.87	15.16	19.05	9.321
111	22.60	393.1	10.98	0	0	1.000	0.2905	0	0
200	25.56	348.2	8.300	11.26	1.668	33.30	7.312	4.219	1.013
002	27.30	326.4	7.145	784.0	100.0	529.0	100.0	484.0	100.0
210	28.64	311.4	6.409	0	0	1.000	0.1696	0	0
201	29.04	307.2	6.211	0	0	15.08	2.478	21.13	3.795
102	30.21	295.5	5.682	0	0	22.19	3.336	31.79	5.223
211	31.81	281.1	5.072	7.093	0.6422	5.852	0.7853	7.093	1.040
112	32.89	272.1	4.717	4.000	0.3368	7.000	0.8736	4.000	0.5456
220	36.46	246.2	3.824	4.000	0.2731	7.000	0.7082	4.000	0.4423
202	37.75	238.1	3.587	11.26	0.7210	33.30	3.160	4.219	0.4376
300	38.76	232.1	3.425	0	0	7.000	0.6343	9.000	0.8914
221	39.07	230.4	3.380	7.093	0.4280	1.000	0.08942	0	0
212	39.98	225.3	3.257	0	0	1.000	0.08617	0	0
310	40.95	220.2	3.144	11.26	0.6320	5.566	0.4630	11.26	1.024
301	41.24	218.7	3.112	208.0	11.56	139.0	11.44	133.0	11.97
003	41.46	217.6	3.090	0	0	25.00	2.044	36.00	3.217

311	43.33	208.7	2.930	0	0	1.000	0.07752	0	0
103	43.54	207.7	2.915	29.65	1.543	33.87	2.612	19.05	1.606
113	45.54	199.0	2.804	0	0	1.000	0.07419	0	0
222	46.14	196.6	2.780	4.000	0.1985	7.000	0.5149	4.000	0.3216
320	47.01	193.1	2.754	11.26	0.5536	1.000	0.07286	0	0
302	48.06	189.2	2.735	0	0	7.000	0.5065	9.000	0.7118
321	49.15	185.2	2.728	29.65	1.444	21.58	1.558	29.65	2.339
203	49.34	184.5	2.728	0	0	15.08	1.088	21.13	1.667
312	49.91	182.6	2.730	11.26	0.5488	5.566	0.4020	11.26	0.8889
213	51.17	178.4	2.748	7.093	0.3480	5.852	0.4255	7.093	0.5636
400	52.52	174.1	2.785	7.093	0.3526	1.837	0.1354	6.731	0.5421
410	54.27	168.9	2.861	0	0	1.000	0.07569	0	0
401	54.50	168.2	2.874	0	0	1.723	0.1310	1.086	0.09025
322	55.21	166.2	2.915	0	0	1.000	0.07712	0	0
330	55.97	164.1	2.965	784.0	41.50	529.0	41.50	484.0	41.50
411	56.21	163.5	2.982	4.000	0.2129	1.000	0.07890	4.000	0.3449
004	56.33	163.2	2.990	784.0	41.85	529.0	41.85	484.0	41.85
223	56.38	163.0	2.995	0	0	1.000	0.07924	0	0
331	57.88	159.2	3.117	0	0	25.00	2.062	36.00	3.245
104	58.00	158.9	3.128	0	0	22.20	1.837	31.79	2.875
303	58.05	158.8	3.133	208.0	11.63	139.0	11.52	133.0	12.05
420	59.29	155.7	3.256	29.65	1.723	21.58	1.859	29.65	2.792
114	59.63	154.9	3.292	4.000	0.2351	7.000	0.6097	4.000	0.3808

313	59.69	154.8	3.298	0	0	1.000	0.08726	0	0
402	60.19	153.6	3.355	7.093	0.4248	1.837	0.1631	6.731	0.6530
421	61.13	151.5	3.471	0	0	1.000	0.09183	0	0
412	61.79	150.0	3.558	0	0	1.000	0.09413	0	0

Table S7 The diffraction peaks and corresponding assignments in high resolution XRD patterns.

hkl	2θ /° (50% P)				2θ /° (80% P)		
	N-10	N-25	N-50	W-10	N-10	N-25	N-50
defect	6.19555	6.19555	6.24537	6.19555	6.19555	6.14574	6.34500
melon		11.1272	11.1272	11.0774	11.1272	11.0744	11.2268
100	12.3726	12.3726	12.4224	12.3726	12.3228	12.3726	12.4722
001	Broad	13.6678	13.8172	13.3689		13.7674	13.8670
101				17.7027	17.6529	17.6031	17.7027
110		18.4002	18.5496				
111		22.1861	22.2857			22.1363	22.2857
200	25.5735	25.3742	25.4240	25.6233	25.6731	25.6233	25.4240
002	27.5162	27.4166	27.5661	27.317	27.6657	27.5661	27.3668

References

1. H.-J. Li, D.-J. Qian and M. Chen, *ACS Appl. Mater. Inter.*, 2015, **7**, 25162.
2. B.-W. Sun, H.-J. Li, H.-y. Yu, D.-J. Qian and M. Chen, *Carbon*, 2017, **117**, 1.
3. H. J. Li, B. W. Sun, L. Sui, D. J. Qian and M. Chen, *Phys. Chem. Chem. Phys.*, 2015, **17**, 3309.
4. A. Savitzky and M. J. Golay, *Anal. Chem.*, 1964, **36**, 1627.
5. A. R. Stokes, *Proc. Phys. Soc.*, 1948, **61**, 382.
6. W. Rachinger, *J. Sci. Instrum.*, 1948, **25**, 254.
7. E. Horvath-Bordon, E. Kroke, I. Svoboda, H. Fueß, R. Riedel, S. Neeraj and A. K. Cheetham, *Dalton T.*, **2004**, 3900.
8. L. Alexander, *J. Appl. Phys.*, 1954, **25**, 155.